



## Deriving original nodule size of lithic reduction sets from cortical curvature: An application to monitor stone artifact transport from bipolar reduction

Matthew Douglass<sup>a,b,\*</sup>, Benjamin Davies<sup>c</sup>, David R. Braun<sup>d</sup>, J. Tyler Faith<sup>e,f</sup>, Mitchell Power<sup>e,g</sup>, Jonathan Reeves<sup>h</sup>

<sup>a</sup> College of Agricultural Science and Natural Resources, University of Nebraska-Lincoln, Lincoln, NE 68583, USA

<sup>b</sup> Agricultural Research Division, University of Nebraska-Lincoln, Lincoln, NE 68583, USA

<sup>c</sup> Department of Anthropology, University of Utah, USA

<sup>d</sup> Center for the Advanced Study of Human Paleobiology, Department of Anthropology, The George Washington University, Washington, DC, USA

<sup>e</sup> Natural History Museum of Utah, University of Utah, Salt Lake City, UT, USA

<sup>f</sup> Department of Anthropology, University of Utah, Salt Lake City, UT, USA

<sup>g</sup> Department of Geography, University of Utah, Salt Lake City, UT, USA

<sup>h</sup> Technological Primates Research Group, Max Planck Institute for Evolutionary Anthropology, USA



### ARTICLE INFO

#### Keywords:

Bipolar reduction

Quartz

Experimental archaeology

Technological organization

### ABSTRACT

Stone tools represent the largest source of information about past human behaviors on the planet. Much of the information about stone tools remains untranslated because we have little understanding about what the variation in artifact form means. One component of stone tool production that has less ambiguity is the reductive nature of the technology. Models of reduction rely on the ability to predict patterns of the rate of mass lost during artifact production. However, these patterns can vary quite substantially due to a variety of factors, one of which is variation in the original size of stone nodules prior to reduction. Here we report on a novel method to estimate the original size of stone nodules based on measurement of the curvature of residual cortex on flake and core products. Using experimental quartz bipolar reduction sets, we demonstrate the suitability of the approach, even when reduction intensity is high. Computer simulation with the experimental sets is then used to demonstrate the method's utility for supporting archaeological inferences about land use and mobility from the analysis of bipolar assemblages. The bipolar flaking method is a technique that was used widely across the 3 million years of paleolithic tool production, yet analytically has received less attention than other modes of reduction. Methods developed here will help to expand understanding for this analytically challenging technological context.

### 1. Introduction

Lithic assemblages produced from small cobbles and pebbles present a challenge to researchers who study assemblages of stone tools. These assemblages are often associated with bipolar reduction where rapid production and the sheer abundance of artifacts created can be formidable for analysis. Often the variability in fracture patterns associated with this technique complicates the identification of basic attributes (Proffitt and de la Torre, 2014), especially for shatter-prone materials like quartz. Despite these difficulties, the global prevalence of this technology warrants detailed investigation.

Small nodule reduction using the bipolar technique has been

recorded across the globe (e.g., de la Peña, 2015a; Hiscock, 2015; Lin et al., 2016; de Lombera-Hermida et al., 2016; Borrazzo, 2012; Jeske and Lurie, 1993), appearing in some of the earliest assemblages (Diez-Martín et al., 2011; Mgeladze et al., 2011) up through the historic (Knight, 1988; Kuijt and Russell, 1993) and indeed the recent/modern era (Arthur, 2010; Hayden, 2015). Yet, analytically, bipolar assemblages have not received as much attention as free hand and bifacial reduction. The literature has largely focused on description of the technique, its variations, and how it might be distinguished from other approaches archaeologically (Gurtov and Eren, 2014). A spate of recent studies, however, have now expanded investigation to consider the technique's relationship to specific raw materials (e.g., Eren et al., 2013; de la Peña,

\* Corresponding author at: College of Agricultural Science and Natural Resources, University of Nebraska-Lincoln, Lincoln, NE 68583, USA.

E-mail addresses: [mdouglass3@unl.edu](mailto:mdouglass3@unl.edu) (M. Douglass), [jfaith@nhmu.utah.edu](mailto:jfaith@nhmu.utah.edu) (J. Tyler Faith).

2015b; Gurtov et al., 2015), the range of products produced (e.g., Kuijt et al., 1995; Bradbury, 2010; Driscoll, 2011; Pargeter and Eren, 2017), and the utility and economy of the method (e.g., Sanchez-Yustos et al., 2015; Pargeter and de la Peña, 2017). Building on these advances, it is important to now consider how analysis of bipolar assemblages can support the development of inferences about technological organization, mobility, and land use (Nelson, 1983).

Here we outline an approach for quantifying original nodule size through the measurement of the curvature of reduced quartz cobbles and pebbles. Remnant traces of the outer cortical surface retained on flakes, cores, and fragments provide a glimpse of the former shape and size of the nodule prior to reduction. Using this curvature and an adaptation of an instrument originally developed for measuring the sphericity of optical lenses, we assess the accuracy with which original nodule size can be determined from experimental quartz assemblages. We employ these estimates to investigate the use of a now-standard measurement of technological organization called the cortex ratio (Dibble et al., 2005; Douglass et al., 2008; Lin et al., 2016; Holdaway et al., 2015) to assess the completeness of bipolar reduction sequences for the study of artifact transport and land use. Results point to the broad suitability of curvature measurement for determining original nodule size for lithics produced from cortical nodules. Results also highlight how variation in raw material flakeability, nodule size, and their subsequent effects on the morphology of reduction products influence the ability to perceive the effects of artifact selection and removal. These observations highlight the need for contextualization of lithic indices to the unique circumstances of any given study region or set of raw material characteristics (e.g., Holdaway and Douglass, 2012; Andrefsky, 1994). Finally, though developed as a solution to issues encountered in bipolar reduction, further evaluation of curvature measurement with a broader array of nodule shapes and sizes, and with different modes of reduction, is warranted.

## 2. Background to the study

The basic definition of bipolar reduction is to put a nodule on an anvil and strike it with a hammerstone (Crabtree, 1972). Others have emphasized variation in how the technique was executed. Callahan (1987), for instance, drew a distinction between bipolar and anvil reduction, with the former having force directed straight downward and perpendicular to the core top and anvil, while the latter reflected force being directed obliquely or away from the point of contact with the anvil. Hiscock (2015) similarly differentiates between a “weak” definition that includes any instance where cores are rested on anvils for reduction, and a “strong” definition reflecting immobilization of a core on an anvil, a direct near 90° angle of blow, and compression of that core during each blow. Beyond definitional constraints, there has also been considerable debate about the intended outcome of the technique (e.g., to produce flakes from cores or to produce special wedge tools). There is considerable difficulty in identifying the products of this technique and distinguishing it from other methods (e.g., direct freehand percussion) (see Shott, 1989; Proffitt and de la Torre, 2014).

Though used on virtually all varieties of source material, bipolar reduction is particularly common with quartz. This can be reasonably attributed to the constraints recognized in working with this material (Knight, 1988; Gurtov and Eren, 2014). Quartz tends to shatter and fragment and is often hard to initiate flake propagation – a factor that is exacerbated with smaller cobbles and pebbles (e.g., Douglass and Holdaway, 2016; Holdaway and Douglass, 2015; Driscoll, 2011; Orton, 2004). Comparative experiments have indicated that the efficiency of bipolar reduction on quartz is not appreciably lower than that obtained through freehand reduction (e.g., Diez Martin et al., 2010) and in fact may produce more complete flakes (Tallavaara et al., 2010; Pargetter and de la Peña, 2017) and enable greater core use intensity (Gurtov and Eren, 2014; Hiscock, 2015; Flenniken and White, 1985; Pargeter, 2016). Combined, these observations indicate that bipolar reduction represents

a rapid way to obtain usable edge from a difficult raw material. This likely underscores the use of this technique across many geographic areas throughout prehistory.

Analytically, the use of bipolar reduction has been related to a variety of different contextual circumstances. It has been argued to reflect limited investment in technology – i.e., an easy way of generating usable edge (e.g., Hayden, 1980), a technique suitable for those possessing limited skills (e.g., Patterson, 1979), an outcome of increased sedentism (e.g., Jeske, 1992), or a reflection of the need for economization of raw material (e.g., Barham, 1987). It is also noted to be particularly common in contexts where the available lithic raw materials are predominantly represented by difficult to work gravels and pebbles (see Shott, 1999 and references therein). Expanding the interpretive framework of this oft used technique especially in instances where small nodules dominate the available raw material is a primary goal of the experimental work we describe here.

## 3. Experimental design

The experiment described here had two purposes: 1. To evaluate the potential for estimating the original size of unworked nodules from the measurement of cortical curvature on stone artifacts, and 2. To evaluate the use of these estimates when calculating the cortex ratio for bipolar assemblages by simulating the selective removal of artifacts at different intensities.

Recently, there has been substantial progress in investigating indices of assemblages that exploit the geometric characteristics of rocks used to make stone tools in order to identify patterns of past behavior. Some geometric attributes can provide an estimate of the dimensions and number of nodules reduced, as well as the proportions of cortex and volume that these nodules had prior to reduction (Dibble et al., 2005; Douglass et al., 2008; Douglass et al., 2018; Douglass, 2010; Phillipps, 2012; Phillipps and Holdaway, 2015; Ditchfield et al., 2014; Lin et al., 2016; Lin et al., 2019; Reeves, 2019). Such an approach establishes a basis for developing natural units (average cobble of set size, volume, and cortex) with which to consider expected material proportions in assemblages. An analogy can be made with faunal analysis, where all the elements of one species in an assemblage can be assessed with respect to natural proportions (e.g., one cranium, two femora, seven cervical vertebrae) and element quantities and deviations in proportions are used to support inferences about number of individuals represented, processing and carcass transport, and by extension land use (e.g., Binford, 1981; Faith, 2007; Faith and Gordon, 2007). Likewise, imbalances between observed and expected geometric attributes are spatially bound, such that artifacts removed from one location are discarded in another (Knell, 2012). Variation in the areal sample of analysis (Openshaw, 1983) influences the ability to perceive the effects of transport and movement under different conditions of human mobility (e.g., frequency, extent and tortuosity) and by extension provide a mechanism for understanding land use through the analysis of different spatial samples (Davies et al., 2018; Douglass, 2010; Rezek et al., 2020; Holdaway, in press). Geometric approaches thus provide a quantifiable expression of the effects of assemblage completeness for fractured stone and by extension support investigation of artifact transport and movement into and out of locations where artifacts are produced.

In the case of bipolar assemblages of small cobbles and pebbles, the degree of fragmentation of cores and flake products presents a further challenge. The geometric approaches mentioned above are based on an understanding of the original shape and size of the nodules from which artifacts are produced. This is complicated by the large quantities of pieces produced using this technique and the ambiguity of flaking attributes produced by bipolar reduction (Proffitt and de la Torre, 2014). Estimates of original nodule size based on counting cores (see Dibble et al., 2005) or measuring core attributes (for flake scar count, see Braun, 2006; Douglass, 2010; for cortex proportion, see Douglass, 2010; Douglass et al., 2018; for upper quartile core size, see Lin et al., 2016) to

infer reduction intensity are not well suited to the core forms typical of bipolar reduction. However, when produced from cortical nodules, the curvature of the remnant cortical surface can be found on the products of bipolar reduction (i.e., cortex or other weathering provides the ability to discern the exterior surfaces of the original nodule). Developing a measure of this remnant curvature on fragments thus provides an opportunity for understanding the average size and shape of original whole nodules that were reduced.

### 3.1. Nodule curvature and its measurement

Measurement of the curvature of fragments to estimate the size and shape of the original whole is an established approach in the study of artifacts. In ceramic analysis, archaeologists have routinely used graduated circles to determine the circumference and profile curvature of pottery sherds, and have extrapolated from these to provide estimates of vessel volume (Whallon, 1969; Egloff, 1973; Hagstrum and Hildebrand, 1990). The curvature on the exterior surface of cortical cobbles/pebbles varies, with some areas being flatter and reflecting more gradual curves than others, some being well rounded, and some areas having greater angularity. However, these differences can be conceptualized as representing a composite surface of numerous spheres of varied sizes, with flatter areas reflecting larger spheres while more curved/angular areas would reflect smaller spheres. This is well known in studies of geometry

where the average of the major and minor axes of an ellipse can be represented as the radius of a single circle of equal area (and volume for ellipsoids and equivalent sphere). Using similar geometric reasoning it is possible to utilize multiple measures of the curvature (i.e., radius of curvature) along a nodule's surface to determine the average curvature and represent this composite value as a single sphere. Measures from many cobbles/pebbles and fragments can likewise be averaged to understand the generalized shape and size of a group.

To measure the curvature of nodules and fragments, we utilized a form of spherometer. Spherometers were originally developed to assist in the production and quality control of hand ground lenses and have found similar application in manufacturing and optometry (Warner, 1998). Traditional spherometers consist of three legs positioned in a triangle with a screw in the middle where the difference in height between legs and middle screw reflects the radius of curvature of a sphere. Two-legged spherometers, are better suited for measurement of aspherical objects and in optometry are referred to as lens clocks, though these often provide measurement in optical power (diopters) rather than measured distance. An earlier archaeological study demonstrated the use of the instrument for measurement of the bulb of percussion for stone flakes (Partel and Ohel, 1981).

The lens clock used for our study was made using a digital indicator consisting of a spring-pressured probe where the distance of plunge is displayed on a digital dial face. A drill press was used on a small block of

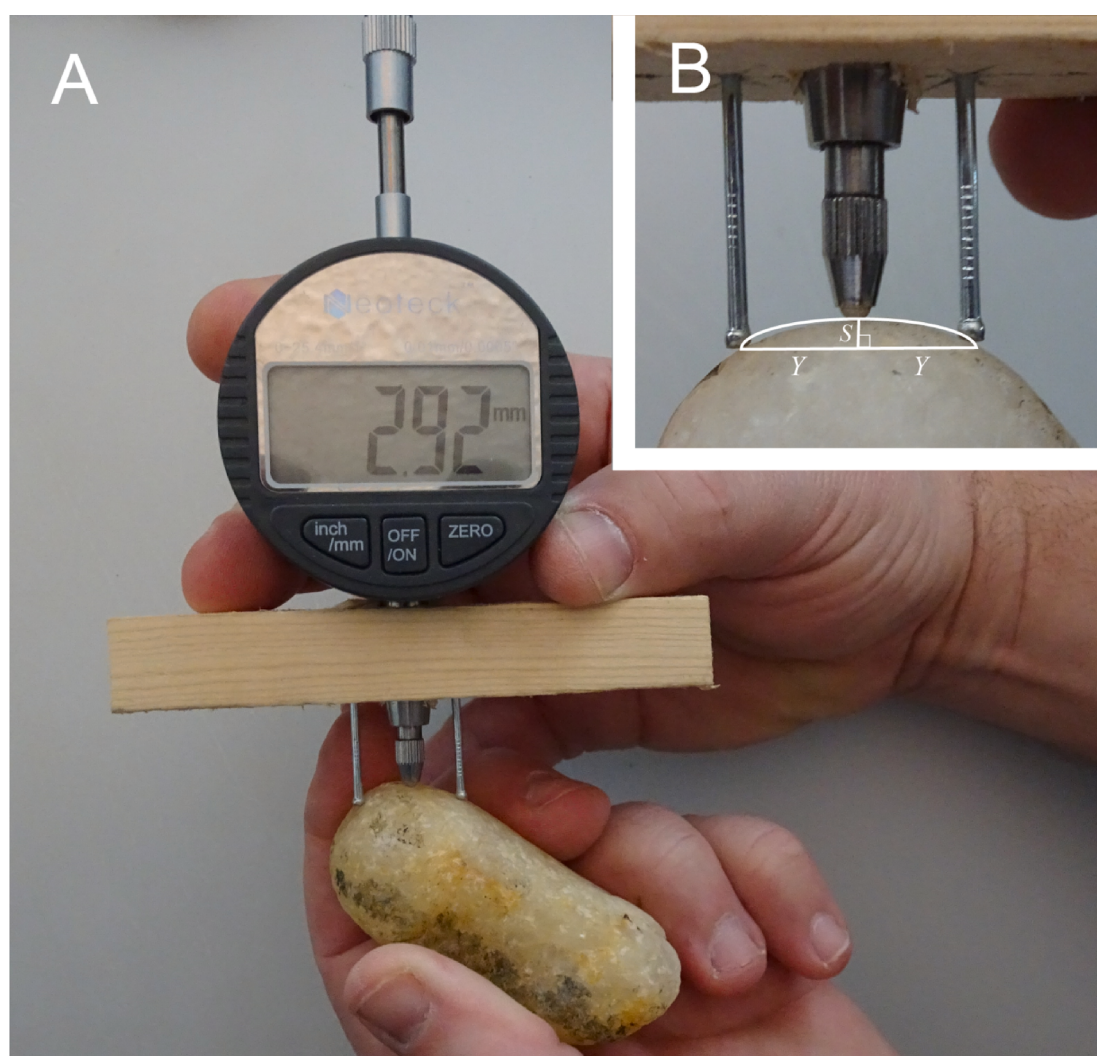


**Fig. 1.** Illustration of Lens Clock developed in this Study. A. demonstrates measurement of cortical curvature with lens clock, note leg position indicating starting point of measure at nodule "end". B close-up image showing derived measures from lens clock used to estimate radius of curvature.

wood to make three holes, one through the block for inserting the probe and two of the same depth and placed equidistant on either side of the central hole in which small brad nails were placed (Fig. 1). Combined, the holes are aligned in a straight row and plumb to the wood block with the probe slightly higher than the two legs. The instrument is zeroed by placing it on a flat surface and holding it vertically so that both legs and probe are of the same height. When placed on a round surface, the legs remain constant while the probe is plunged inward. The equation for the radius of curvature is

$$r = \frac{y^2 + S}{2S} + \frac{S}{2}$$

where  $y$  equals the distance between each leg and the probe tip (half the distance between legs) and  $S$  equals the distance from zero traveled by the probe (Fig. 1).

Lens clock readings were then taken over the cortical surface of all nodules prior to reduction, and all cortical fragments produced during knapping. With spherical surfaces, lens clocks will provide the same measurement at any orientation. Aspheric surfaces are not uniform and thus will produce different measurements over the same surface depending on the instrument's orientation. This is the same issue noted for pottery where separate profile and axial measurements of curvature are made (Whallon, 1969). In the use of the lens clock, we adopted a similar approach where two separate measures were made – first oriented to the longest axis of the core or fragment and then perpendicular to this initial axis. Working with one orientation (the A axis for cobbles, cores and cortical portions of flakes and fragments), separate measurements were taken over the artifact's cortical surface at approximately 1 cm increments in a grid-like fashion. This same process was then repeated in the same 1 cm grid pattern but at the perpendicular orientation. All measures are then averaged to determine a mean curvature measurement. This mean curvature measurement is directly proportional to the average radius of the cobble.

There are a few caveats that deserve mention to help operationalize curvature measurement in the experimental test case. These were derived through initial testing with separate nodules and fragments prior to completion of the study. Adoption of the approach should likewise trial measurements on known test cases (i.e., known cobbles/pebbles and fragments) to avoid measurement error that would unduly influence the resultant estimate of nodule size. These caveats are as follows. First, pits or other depressions on the surface were not measured, but instead replaced with measurements on adjacent areas. This is to eliminate negative values of  $S$  in the readings. Likewise, flat areas (zero to slightly negative) were given values of 0.1 again to eliminate negative values. The justification for this decision was that we were interested in the "positive curvature" of the cobbles for estimates of original size. In a similar fashion, cortical surfaces for flakes and flake fragments were often too narrow to complete perpendicular measurements. In instances where surfaces were nearly large enough, measurements in the second round were at times taken slightly off of perpendicular. Finally, it should be noted that with bipolar reduction, there is a tendency to strike the nodule along the long axis, hitting it at its most acute point. This often results in crushing of platforms and obliteration of areas that would reflect the smallest radius of curvature over the entire nodule. As a result, platform areas often reflect the greatest curvature on a flake produced using bipolar reduction. Likewise, flake margins and terminations are often found along the areas of steeper cortical curvature (e.g., along edges on elliptical and angular parts of nodules). To accommodate this issue, effort was made to abut one leg of the lens clock on the outer edge (i.e., lip) of cortical surface when starting measurement so as to account for this underrepresented area of remnant nodule surface. With less spherical and more ellipsoidal cores and unworked nodules, different surfaces or "faces" were measured with division being made on the rounded "end" of the artifact (e.g., vertex of an ellipsoid). Thus the lens clock leg began at the "end" of

each side/surface of a nodule (see Fig. 1A). Summary information of the experimental data is presented in Tables 1, 2, and 3.

### 3.2. Experimental materials

Twenty alluvial quartz pebbles derived from gravel extraction pits in eastern Nebraska were obtained from a landscaping supply store. Selection was based on the need to incorporate a range of shape variation found naturally among the alluvial quartz pebbles, and to gauge lens clock suitability for an array of irregular pebble shapes and sizes. As such, the experimental pebbles show considerable variation in shape but were generally sub-rounded to well rounded (Powers, 1953) (Fig. 2). Pebble mass ranged from 53 to 252 g. Weight, metric dimensions, curvature (from lens clock), cortex proportion (using the equations for the surface area of a scalene ellipsoid and a sphere; see Douglass et al., 2008), and volume (weight/ specific gravity (2.53 from a sample of the experimental cores; Mueller, 1977) were recorded for each unworked pebble (Table 1). Reduction proceeded using the bipolar technique on a quartzite anvil using a quartzite hammerstone. There was noted core splitting (likely because of irregularities in the quartz matrix) for many of the pebbles. To address this effect, two separate datasets were developed. One reflected initial reduction that was suspended once a pebble became fragmented, while the other consists of eight of the quartz pebbles that were subject to further, more intensive, reduction of fragments (i.e., multiple cores per nodule). This approach provides a measure of the effects of reduction intensity on the measures employed in the study.

### 3.3. Experimental data and Summary information

Table 1 presents baseline data for the experimental quartz nodules, as well as comparison between these measures and estimates of the radius of a sphere of approximate size. The A, B, and C axes of each pebble were measured with calipers and averaged to calculate the mean radius of each pebble. Average lens clock readings ( $S$ ) were used to calculate the radius of curvature (Lens Clock Radius) on both unworked pebbles and resultant reduction sets. In spite of considerable shape variation (i.e., pebbles were far from spherical in most instances; see

**Table 1**  
Experimental pebble attributes. Reduced major axis regression from average radius used to calculate root mean squared error (RMSE), intercept, and slope.

Pebble	Initial Mass (g)	Mean Caliper Radius (mm)	Lens Clock Radius - Whole (mm)	Lens Clock Radius - Knapped (mm)
1	199	26.67	29.03	28.57
2	101	21.17	23.49	26.31
3	80	20.00	21.50	23.94
4	92	21.50	20.80	26.31
5	252	29.67	28.13	31.02
6	181	27.67	24.657	26.89
7	56	18.83	20.06	16.54
8	222	28.67	28.57	27.29
9	53	18.17	21.87	18.22
10	67	19.50	19.75	22.51
11	119	23.17	24.90	27.70
12	184	27.5	26.13	22.78
13	147	26.67	23.94	29.03
14	72	19.17	20.37	25.94
15	107	23.00	22.38	20.16
16	130	24.33	26.70	27.09
17	213	29.17	28.35	27.92
18	92	20.50	20.16	30.75
19	110	24.33	29.99	31.29
20	117	23.00	24.25	27.09
Mean	129.7	23.63	24.25	25.87
RMSE			1.93	3.84
Intercept (95% confidence)			3.59	-0.30
Slope (95% confidence)			0.87	1.10

**Table 2**

Experimental reduction set attributes.

Light Reduction Quartz					Heavy Reduction Quartz			
Pebble	N	Length of smallest artifact (mm)	Average length (mm)	Length of largest artifact (mm)	N	Length of smallest artifact (mm)	Average length (mm)	Length of largest artifact (mm)
1	11	11	31.91	69	—	—	—	—
2	15	12	28.67	54	—	—	—	—
3	13	14	25.46	44	—	—	—	—
4	16	14	25.00	48	—	—	—	—
5	38	12	24.63	53	—	—	—	—
6	18	13	31.78	67	35	11	26.09	65
7	11	12	22.00	43	21	12	20.14	42
8	15	11	29.80	54	43	9	19.65	47
9	7	10	27.71	47	—	—	—	—
10	8	15	29.50	43	44	10	21.39	43
11	16	13	26.50	52	—	—	—	—
12	5	22	41.60	56	46	12	23.20	36
13	20	17	29.20	57	45	1	21.40	53
14	10	13	28.20	47	—	—	—	—
15	13	11	22.54	45	—	—	—	—
16	10	14	32.20	64	—	—	—	—
17	18	13	29.44	77	70	10	21.03	44
18	33	11	18.94	52	—	—	—	—
19	19	10	22.42	54	35	10	21.03	38
20	6	15	38.83	58	—	—	—	—

**Table 3**

Original nodule size and cortex ratio calculations for experimental assemblages.

	Light Reduction Quartz	Heavy Reduction Quartz
<b>Whole assemblage characteristics</b>		
Mass (g)	2524	851.19
Volume (mm <sup>3</sup> )	997.63	336.44
<b>Theoretical nodule estimates</b>		
Radius (mm)	26.06	25.58
Surface area (mm <sup>2</sup> )	85.34	82.22
Volume (mm <sup>3</sup> )	74.13	70.11
<b>Cortex ratio calculations</b>		
Estimated number of nodules	13.46	4.80
Expected cortical surface area (mm <sup>2</sup> )	1148.68	394.66
Observed cortical surface area (mm <sup>2</sup> )	1224.63	439.70
Cortex ratio	1.07	1.11

Fig. 2), the lens clock and sphere equations approximate those obtained using caliper measurement.

Table 2 presents basic information on the resultant reduction sets with two distinct phases of reduction intensity (light and heavy reduction) as well as measures of cortex proportions for the experimental reduction sets. The methods for deriving the cortex ratio have been described in detail elsewhere (e.g., Douglass et al., 2008). To briefly summarize, the measure is based on dividing the total observed cortical surface area against that which would be expected in an assemblage. The expected value is derived from the volume of stone and the average nodule characteristics from which the assemblage was produced. Observed cortical surface area for the assemblage was obtained by multiplying measures of surface area by the proportion of cortex noted on each artifact. Here, surface area was calculated by multiplying the maximum length by the maximum width for all artifacts. Cortex proportion was estimated using 10% increments. Surface area (e.g., 10 cm<sup>2</sup>) and cortex proportions (e.g., 20%) were then multiplied for each artifact producing a measure of cortical surface area (e.g., 2 cm<sup>2</sup>). These were then summed (e.g., 20 flakes with similar values would result in 40 cm<sup>2</sup>) to arrive at total assemblage quantities.

Expected cortical surface area is obtained by first developing an estimate of the average unworked cobbles/pebbles from which an

assemblage is produced. This is termed the “theoretical nodule”. As noted, in other contexts (e.g., free hand reduction) core attributes (e.g., percent cortex, flake scar density) are used to predict average unworked nodule from cores (Douglass et al., 2018). However, given the unique circumstances of bipolar assemblages (e.g., cores are often split and do not accumulate greater scar density with increased reduction), an alternative estimate is needed. To estimate the size of the theoretical nodule with bipolar assemblages, lens clock readings *S* were averaged for all cortex bearing artifacts and then input in the equation for the radius of curvature (see above), which is then input into the equation for the surface area of a sphere.

$$SA = 4\pi r^2$$

and the volume of a sphere

$$V = \frac{4}{3}\pi r^3$$

The result is an estimate of the surface area and volume of the average unworked nodule as derived from cortex curvature from all cortex bearing fragments. The total assemblage volume (mass/specific gravity) (see Douglass et al., 2008) is then divided by the theoretical nodule volume (see above) to determine the number of nodules represented in each assemblage. This value is then multiplied by the surface area of the theoretical nodule (again estimated based on knowledge of expected average nodule size) to produce the expected cortical surface area in an assemblage.

Comparison of cortex ratio values for the two samples indicates close agreement between observed and expected cortex proportions. The light reduction quartz produced a value of 1.07, the heavy reduction quartz a value of 1.11. These slight overestimates of observed cortical surface area to that expected are in line with similar experimental tests of the method’s performance using different materials and reduction techniques (Douglass et al., 2008; Lin et al., 2015). A primary cause of overestimation can be attributed to the use of maximum dimensions in measurement of flake area and by extension cortical surface area. Nevertheless, in archaeological applications there is a tendency for the calculation of cortex ratio to be reflective of a paucity of cortex, likely a result of the selective removal of larger flakes. The slight overestimates of cortex described here (see above) most likely mitigates against false perceptions of higher than expected artifact transport. This generalized overestimate of cortex proportion potentially prevents type one errors.

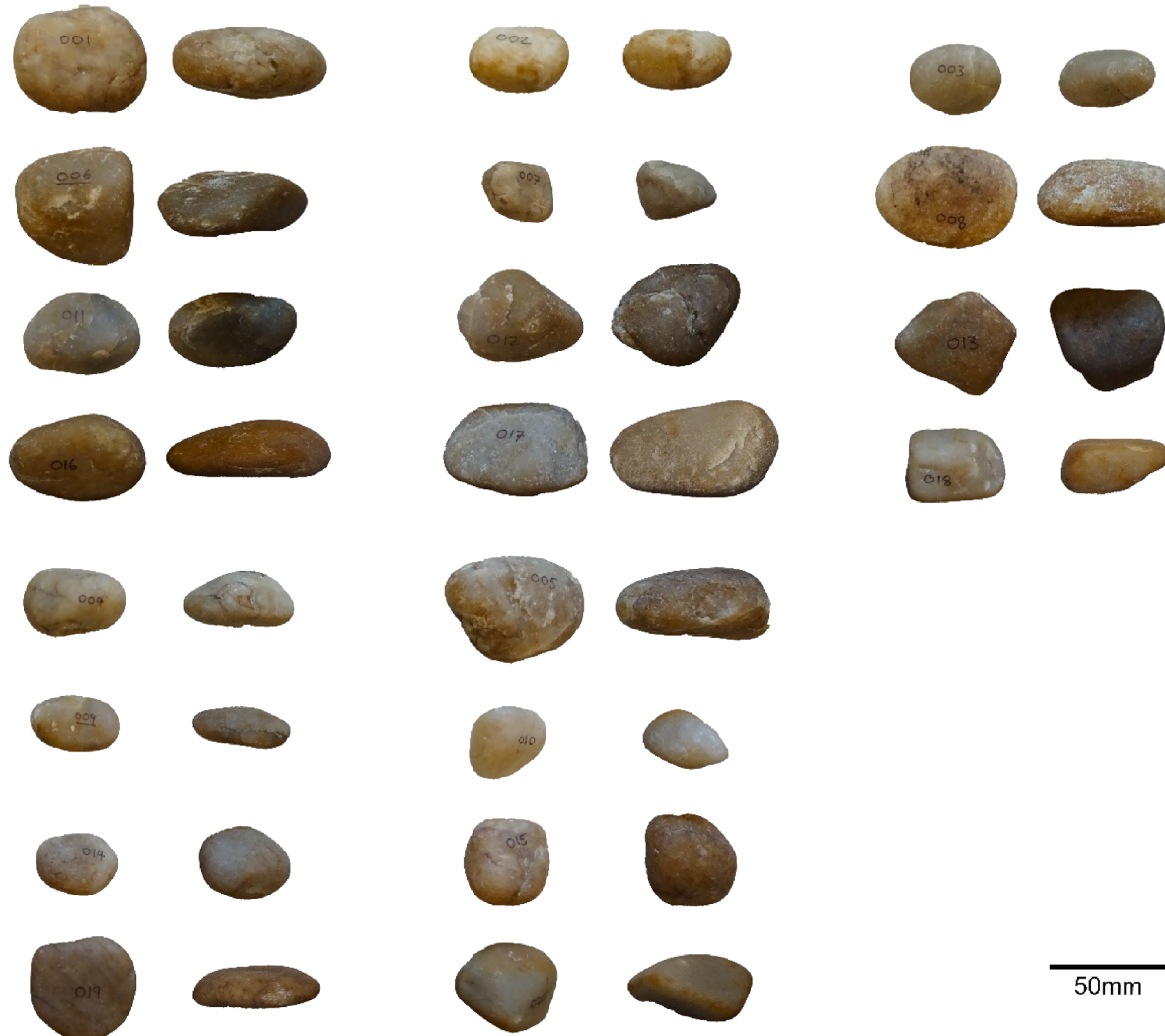


**Fig. 2.** Experimental quartz pebbles. The experimental pebbles were selected to encompass a range of shape and sizes. The sampled pebbles demonstrate considerable variability in degree of angularity, rounding, and eccentricity.

#### 4. Simulating application to archaeological assemblages

Since measures like the cortex ratio are effectively indicators of the removal or addition of geometric attributes to an archaeological assemblage, it is important to understand how well the curvature estimates perform with assemblages composed of products from multiple nodules, as well as instances where some products of reduction have been subtracted or added. Bootstrap simulations were used to generate larger assemblages composed from the reduction products of multiple experimental nodules. Bootstrap approaches have been used in other studies of lithic assemblage formation to address the effects of variability in manufacture and selection on sampling distributions (e.g., Parker, 2012; Lin et al., 2015; Morales, 2016). Simulations were written using the R statistical computing platform (version 3.4.3, R Development Core Team, 2017).

In the simulations, nodules used in the experimental dataset were selected at random, and all the fragments produced from those nodules were added to the simulated assemblage. This process was then repeated with replacement until a desired size  $N$  was reached. From the simulated assemblage, a sample of size  $n$  fragments was drawn at random, and an array of  $S$  values were obtained by combining the lens clock readings  $S$  from those fragments. So, for example, if an assemblage of 10,000 fragments was generated through bootstrap sampling, and a sample of 100 fragments was drawn from that assemblage, and each fragment

contained 20 readings of  $S$ , the resulting sample would contain 2000 readings of  $S$ . In reality, the number of readings of  $S$  varies between fragments, so the number of readings varies depending on which fragments compose the sample. The mean value of these  $S$  readings was then used to obtain the radius and thereafter volume and surface area of a theoretical original nodule, and cortex ratios were then calculated for the simulated assemblage from these.

To assess the effect of fragment sample size to estimate average original nodule size, simulated assemblages of 10,000 fragments were generated, and  $S$  readings from samples of 10, 50, and 100 fragments were used to obtain an estimate of average nodule radius. These values were then compared to the average of the axial radius estimates for all nodules used to generate the simulated assemblage.

The bootstrap approach was also used to simulate assemblages where material has been added or removed. In runs where material has been removed, the simulated assemblage was reduced by a percentage  $R$ ; this variable was explored at 25% and 50% removal. The fragments selected for removal may be drawn randomly, or be removed preferentially based on a given set of 'selection criteria' (e.g., Parker, 2012) to simulate users targeting fragments with particular qualities. In the latter case, fragments are arranged in a descending order that maximizes the criteria (e.g., length), and are then removed in that order until the removal percentage is reached. So, for example, if the selection criterion is length and  $R$  is 50%, the fragments would be ordered on length and

then the longest fragments would be removed in that order until 50% of the total assemblage is removed ( $n \times R$ ). In simulations where material has been added, a percentage  $A$  was used to determine the amount added, again explored at 25% and 50% percent relative to the original assemblage size ( $n \times A$ ). In this case, however, the fragments, either randomly or preferentially selected, are duplicated rather than removed. For both removal and addition scenarios, assemblages of 10,000 fragments provided the initial assemblage, 100 fragments were used to produce an average  $S$  value, and three selection criteria were explored in terms of their effect on the estimate of radius and cortex ratio:

- **None** Fragments are selected at random
- **Flakes Only** Fragments identified as flakes are selected at random
- **Cortical Surface** Fragments are selected based on their absolute cortical surface area
- **Surface Area-to-Volume Ratio** Fragments are selected based on the ratio of surface area to volume (e.g., ‘flatness’)

## 5. Simulation results

### 5.1. Effect of sample size on estimate of average nodule

Since the characteristics of the original nodules used in the generation of the simulated assemblages are known, we estimated the radius size for each of these using axial dimensions ( $l \times w \times t$ ), then took the average of those values and compared them to the average of radius estimates obtained from lens clock measurements using different numbers of fragments in simulated assemblages. Simulations that used low sample sizes ( $n = 10$ ) were more variable in their differences from the average axial estimate of nodule radius. This is because of the broad range in curvature for individual fragments – some being rounded and others flat – and thus the opportunity for outliers to have outsized influence on estimates. Where samples are larger ( $n = 50, 100$ ), values coalesce more tightly around an average value close to parity. This effect of sample size and averaging on the cortex ratio in general has been previously demonstrated by Lin et al. (2010).

Although both reduction sets had averages close to a value of 1, the

average value for the lightly reduced quartz dataset is slightly higher on average (Fig. 3) indicating that the  $S$  (curvature) measurements obtained from that experimental dataset slightly overestimate radial size when compared to axial measurements (~1.09). However, this overestimation is not substantial for the purposes of using geometric methods and would only serve to slightly inflate cortex ratios rather than decrease them (Dibble et al., 2005:552). The average of the heavily reduced assemblage was ~1.01 (Fig. 3).

### 5.2. Estimating average original nodule radius and cortex ratio for incomplete and augmented assemblages

The sensitivity of the cortex ratio to the amount of cortical surface present in the assemblage (i.e., spatial sample) is what makes it useful as a measure of mobility. For applications of the curvature estimate described in this study, the amount of cortical surface present in an assemblage is also important for obtaining an adequate number of lens clock readings to produce an accurate estimate of average original nodule size. Since both of these would likely be affected by the removal or addition of fragments to an assemblage, we added or subtracted fragments to simulated assemblages according to a given selection criterion (e.g., flakes only), and then compared the ratio of curvature-to-axial based estimates of average nodule radius (a measure of the accuracy of the nodule size estimate) to the cortex ratios obtained from the resulting assemblages.

Results from these simulations are displayed in Figs. 4 and 5. Overall, adding fragments has little effect on the accuracy of curvature-derived nodule radius estimates, while subtracting can alter estimates depending on what characteristic is being targeted. This makes intuitive sense, as adding fragments can only increase the number of cortical fragments useful for taking lens clock measurements, while removal has the potential to reduce the number of these fragments thus increasing the effects of outliers. Unsurprisingly, removal based on an explicit preference for cortical surface had the most significant impact on the accuracy of curvature-derived nodule radius estimates. In instances where fragments are removed or added randomly, the effect is negligible on both measures. This is because there is no systematic imbalance created

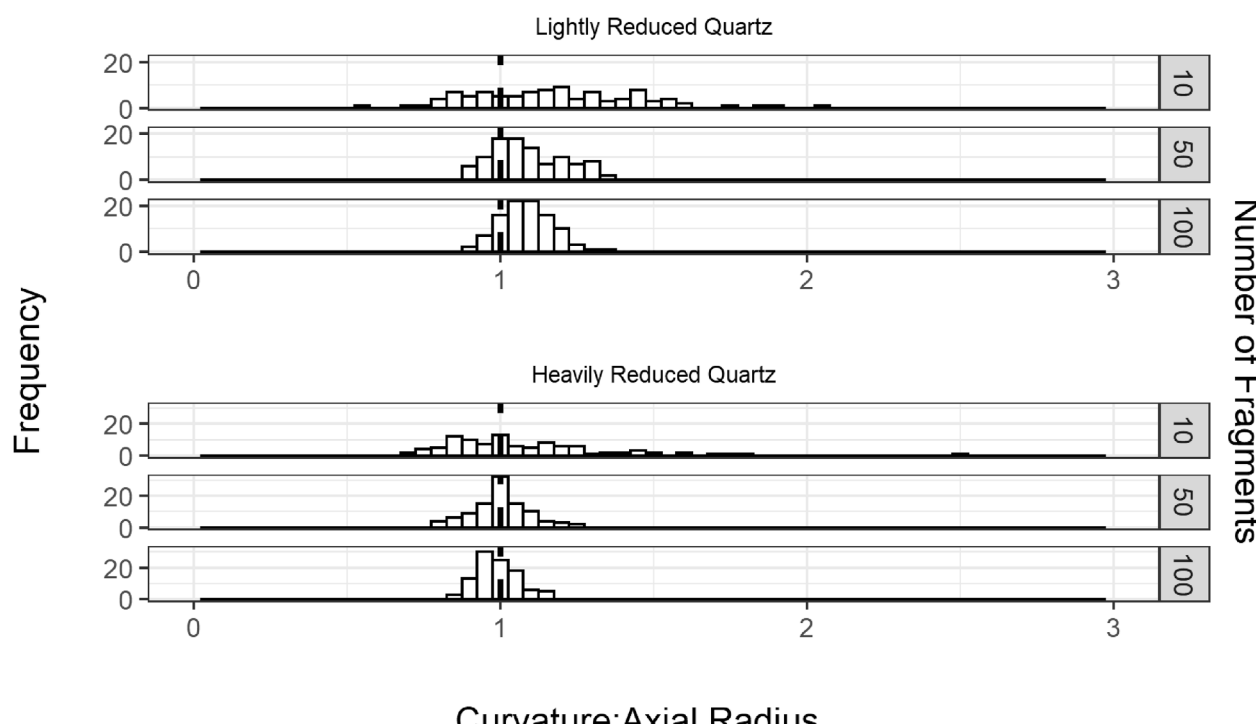


**Fig. 3.** Effect of sample size (number of fragments) on ratio of curvature-derived to axial-derived mean nodule radius estimate for experimental assemblage.

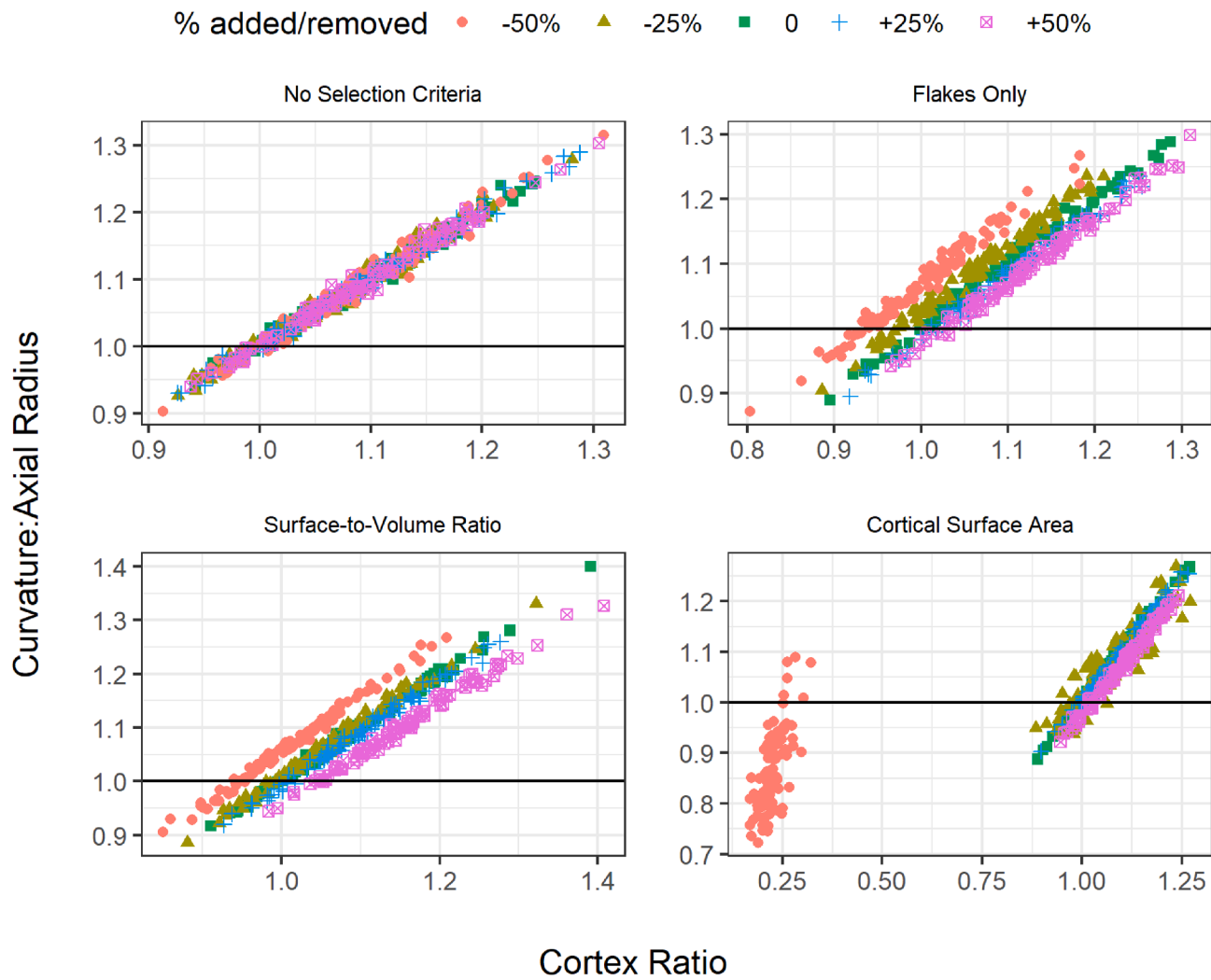


**Fig. 4.** Effects of assemblage augmentation on cortex ratio and curvature-derived average nodule radius for lightly-reduced quartz assemblages.

between cortical surface area and volume as items are removed randomly, and since the estimate of number of original nodules depends on assemblage volume, this value keeps pace with removal or addition (upper left in 4 and 5).

For the most part, the simulations produce expected patterning in cortex ratios, where adding fragments (i.e., flakes, flake fragments, and angular fragments) tends to inflate cortex ratios while removing fragments decreases them. This is particularly clear when fragments are selected for their ratio of surface to volume (lower right in Figs. 4 and 5). However, there are differences among the experimental datasets in terms of capacity to produce this patterning. Selective removal of cortical fragments in the heavily reduced assemblage, for example, produces the expected patterning (lower left in Fig. 5), while the lightly reduced quartz does not show any shift except when 50% of the assemblage is removed (lower left in Fig. 4). This relates primarily to the qualities of the products of reduction in these experimental assemblages. In the case of isotropic materials like chert or flint, bipolar reduction techniques can reliably be used to generate products that are easily distinguished as flakes or cores. Flakes, being thin and flat, may possess a disproportionate amount of cortical surface but almost always represent a limited amount of volume relative to the original nodule. Conversely, cores may possess varying amounts of cortical surface area depending on reduction intensity, but always tend to represent a substantial amount of volume. Separating these two components systematically can affect patterning in the geometric properties of an assemblage that track with the removal or addition of flaked stone.

In the case of bipolar-reduced quartz, the ‘chunky’ nature of the reduction products means that fragments that have a substantial amount of cortical surface may also represent the bulk of the volume in an assemblage. In such an instance, systematically selecting pieces for either volume or cortical surface area may have less predictable effects on the cortex ratio as they are autocorrelated. In the case of the lightly reduced quartz assemblage (Fig. 4), this means that large, voluminous pieces may still carry a substantial amount of cortex, preventing the separation of cortical surface from volume that produces changes in the cortex ratio. By breaking up these larger pieces through continued reduction, the heavily reduced quartz assemblage (Fig. 5) separates cortex from volume more effectively and shows greater differentiation in cortex ratios at different degrees of selection intensity.

## 6. Discussion and conclusion

The results presented in this study indicate that the curvature of cortex on flakes, cores, and fragments can be used to estimate initial nodule size for cortical cobbles and pebbles. Specifically, the lens clock method described above provides an efficient means to accomplish this goal. This finding remains true even when substantial amounts of material are removed from assemblages, although the loss of a significant amount of cortical surface area (50% or more) can inhibit estimates simply by reducing the number of potential sources of lens clock readings. The accuracy of the method improves with more measurements and more pieces measured, and for many archaeological applications it

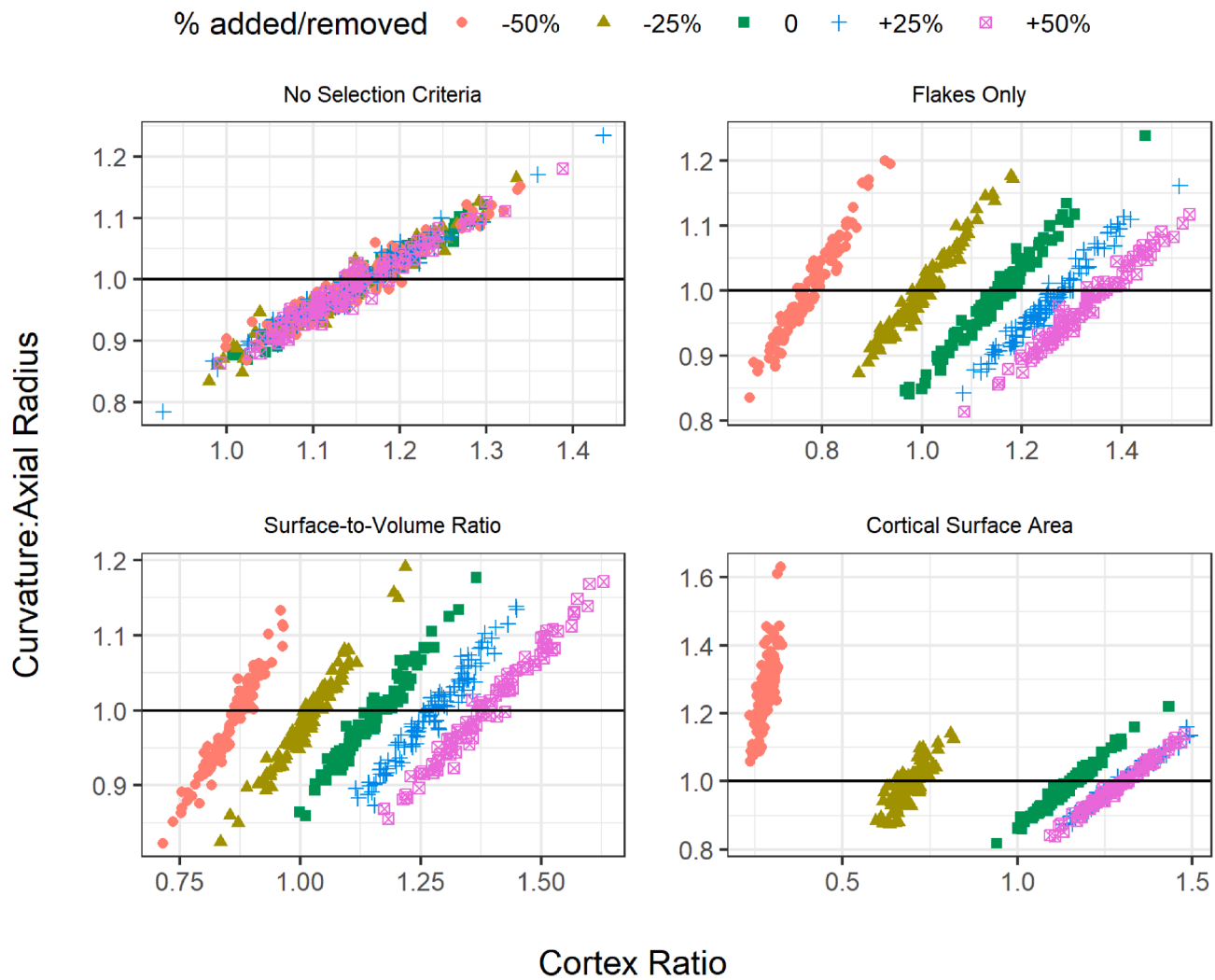


**Fig. 5.** Effects of assemblage augmentation on cortex ratio and curvature-derived:axial-derived average nodule radius for heavily-reduced quartz assemblages.

would be possible and preferable to measure all artifacts within an assemblage. However, it is important to note that an accurate approximation of the original nodule size can be gained with as few as 100 cortical fragments (i.e., the parameter used in this simulation).

While specifically developed to address the issue of bipolar reduction of quartz pebbles, curvature estimate using the lens clock are likely broadly suited to a range of issues where knowledge of initial package size is important. Bigger cobbles allow for larger flakes and more flakes per core, and affect the relationship between reduction intensity and different attributes such as dorsal cortex and flake scar morphology. As such, initial nodule size is a major determinant of assemblage variability and can affect the performance of different lithic indices. The experimental pebbles from this study demonstrated considerable shape and size variation, thus suggesting curvature measurement is broadly scalable to different contexts and indeed indices where cortical pebbles and cobbles were reduced. Further study using different materials (of different size and sphericity/angularity) and modes of reduction is warranted.

The wider goal of this study was to integrate this approach into geometric whole assemblage indicators of past mobility. Applications of the cortex ratio method have provided insights into past patterns of land use around the world. In semi-arid Australia, cortex ratios from middle Holocene surface assemblages repeatedly demonstrate a deficit in cortical surface area (Douglass et al., 2008; Holdaway et al., 2015). This includes a systematic sampling of 94 surface assemblages over a  $15 \times 10$

km dry creek catchment at Rutherford's Creek, which exhibit cortex ratio values distributed around an average of 0.55 (Davies et al., 2018). These patterns have been interpreted to indicate the systematic removal of large and thus overly cortical flakes, indicating extensive mobility in a marginal and unpredictable environment. Similarly, Lin and colleagues (2016) found low cortex ratio values for Pleistocene surface assemblages along the Doring River in South Africa, suggesting the transport of cortical flakes away from the studied area. In Egypt, Phillips (2012) applied a variant calculation based on the ratio of observed-to-expected volume of artifacts (volume ratio) to establish whether the high cortex ratios for Holocene assemblages were the result of an influx of flakes or the removal of cores. Results of this analysis of the cortex and volume ratios were consistent with the hypothesis of transported cores and secondary removal of flakes (see also Phillips and Holdaway, 2015). Further, on the island of Aitutaki in the central Pacific Ocean, Ditchfield et al. (2014) argue that high cortex ratios and low volume ratios from assemblages of basalt artifacts were consistent with the interpretation of regular removal of adze preforms where the cortex had been preferentially removed prior to the transport of these forms. Finally, Holdaway et al., 2015 compared landscape scale measures of cortex between Holocene age Australian and North American Great Plains samples from Nebraska to evaluate the effects of topography and environment on structured land use patterns within the respective study areas. Combined, these studies demonstrate variability in the organization of lithic technology as part of past systems of land use that can be fruitfully

compared using a common methodology.

Up to this point, studies using geometric measures have been limited to instances where nodule size estimates can be made from known raw material variability or core qualities. This study shows that cortex ratios derived from curvature-based estimates of average nodule size can be used in most cases as a reliable indicator of the intensity of removal or addition of cortical surface in assemblages, giving insights into the organization of technological and mobility in the past. This is particularly useful in case studies where access to probable sources is limited (e.g., Douglass and Holdaway, 2011) or where average initial nodule size cannot be easily estimated using core or flake sizes (e.g., Phillipps and Holdaway, 2015; Lin et al., 2016) or measure of core reduction intensity (e.g., Douglass et al., 2018; Braun, 2006). This includes assemblages produced through bipolar reduction, a technique that was widely used in the past by groups who likely had differing approaches to land use and technological organization to those that have already been studied. The ability to include otherwise intractable assemblages expands the applicability of the approach, facilitating comparisons between different technologies, regions, and time periods and improving understanding of the variation in human mobility.

Going forward, the lens clock-based approach to nodule size estimate and its use with the cortex ratio should be explored broadly with different pebbles/cobbles from different locations. Nodule shape and size and in fact reduction intensity will affect how the method performs. Experimental applications should be used to verify and calibrate the approach to account for this variability. The size and spacing of the distance between legs on the instrument and density of readings should also be adjusted to suit contextual needs. For example, a smaller leg spacing on the instrument and smaller measurement intervals should be used for pebbles smaller than those used in the experimental assemblage.

This study provides a basis for more detailed study of bipolar reduction and increased research opportunity for any assemblages derived from cortical pebbles/cobbles. Because of the widespread use of bipolar reduction (especially with small water worn cobbles and pebbles), comparison will help to clarify how products of this technology are transported in different contexts and indeed between different technologies. Incorporating simulation of artifact transport and discard using different technologies (e.g., bipolar quartz pebble reduction and free-hand reduction of large cobbles of more easily flaked materials) can help to establish linkages between archaeological measures and behaviors affecting lithic assemblage composition in the past (e.g., Barton and Riel-Salvatore, 2014; Davies, 2018; Coco et al., 2020). Greater effort at understanding how different materials and package sizes influence signatures of reduction, use, and transport is critically important.

## Declaration of Competing Interest

The authors declare that they have no known competing financial interests or personal relationships that could have appeared to influence the work reported in this paper.

## Acknowledgement

This study was supported by NSF# 1826666 and NSF# 1924322. We thank Andrew Kandel and two anonymous reviewers who provided helpful comments on earlier drafts of the manuscript.

## Data availability statement

The data that support the findings of this study are openly available via an MIT License in Zenodo at <http://doi.org/10.5281/zenodo.4074199>, reference number 4074199.

## References

- Andrefsky, W., 1994. Raw-material availability and the organization of technology. *Am. Antiq.* 59, 21–34.
- Arthur, K.W., 2010. Feminine knowledge and skill reconsidered: women and flaked stone tools. *Am. Anthropol.* 112 (2), 228–243. <https://doi.org/10.1111/j.1548-1433.2010.01222.x>.
- Barnham, L.S., 1987. The bipolar technique in Southern Africa: a replication experiment. *South Afr. Archaeol. Bull.* 42 (145), 45–50. <https://doi.org/10.2307/3887773>.
- Barton, C.M., Riel-Salvatore, J., 2014. The formation of lithic assemblages. *J. Archaeol. Sci.* 46, 334–352. <https://doi.org/10.1016/j.jas.2014.03.031>.
- Binford, L.R., 1981. *Bones : Ancient Men and Modern Myths. Studies in Archaeology*. Academic Press, New York.
- Borrazzo, K.B., 2012. Raw material availability, flaking quality, and hunter-gatherer technological decision making in Northern Tierra Del Fuego Island (Southern South America). *J. Archaeol. Sci.* 39 (8), 2643–2654. <https://doi.org/10.1016/j.jas.2012.03.018>.
- Bradbury, A.P., 2010. Bipolar reduction experiments and the examination of middle archaic bipolar technologies in West-Central Illinois. *North Am. Archaeol.* 31 (1), 67–116. <https://doi.org/10.2190/NA.31.1.d>.
- Braun, D.R., 2006. The Ecology of Oldowan Technology: Perspectives from Koobi Fora and Kanjera South. Ph.D. Dissertation, New Brunswick, NJ, Rutgers The State University of New Jersey.
- Callahan, E., 1987. An evaluation of the lithic technology in Middle Sweden during the Mesolithic and Neolithic. *Societas Archaeologica Upsaliensis*.
- Coco, E., Holdaway, S., Iovita, R., 2020. The effects of secondary recycling on the technological character of lithic assemblages. *J. Paleol. Archaeol.* 3 (3), 453–474. <https://doi.org/10.1007/s41982-020-00055-4>.
- Crabtree, D., 1972. An Introduction to Flintknapping. *Occasional Paper of the Idaho State University Museum* 28.
- Davies, B., 2018. Weaving the Common Threads of Formation and Simulation. *Exploring Oceans of Data: Papers from the 44th Conference on Computer Applications and Quantitative Methods in Archaeology*. University of Oslo, Oslo.
- Davies, B., Holdaway, S.J., Fanning, P.C., 2018. Modeling relationships between space, movement, and lithic geometric attributes. *Am. Antiq.* 83 (3), 444–461. <https://doi.org/10.1017/aqc.2018.23>.
- Dibble, H.L., Shurmans, U.A., Iovita, R.P., McLaughlin, M.V., 2005. The measurement and interpretation of cortex in lithic assemblages. *Am. Antiq.* 70, 545–560.
- Diez-Martin, F., Sanchez Yustos, P., Dominguez-Rodrigo, M., Mabulla, A.Z.P., Bunn, H.T., Ashley, G.M., Barba, R., Baquedano, E., 2010. New insights into hominin lithic activities at FLK North Bed I, Olduvai Gorge, Tanzania. *Quarter. Res. Paleocoll. Hominin Behav. Bed I at Olduvai Gorge (Tanzania)* 74 (3), 376–387. <https://doi.org/10.1016/j.yqres.2010.07.019>.
- Diez-Martin, F., Yustos, P.S., Domínguez-Rodrigo, M., Prendergast, M.E., 2011. An experimental study of bipolar and freehand knapping of Naibor Soit Quartz from Olduvai Gorge (Tanzania). *Am. Antiq.* 76 (4), 690–708. <https://doi.org/10.7183/0002-7316.76.4.690>.
- Ditchfield, K., Holdaway, S.J., Allen, M.S., McAlister, A., 2014. Measuring stone artefact transport: the experimental demonstration and pilot application of a new method to a prehistoric Adze Workshop, Southern Cook Islands. *J. Archaeol. Sci.* 50 (October), 512–523. <https://doi.org/10.1016/j.jas.2014.08.009>.
- Douglass, M.J., 2010. The Archaeological Potential of Informal Lithic Technologies: A Case Study of Assemblage Variability in Western New South Wales, Australia. Ph.D. Dissertation, Auckland: The University of Auckland.
- Douglass, M.J., Holdaway, S.J., 2011. Changing perspectives in Australian archaeology, Part IV: Quantifying stone raw material size distributions: investigating cortex proportions in lithic assemblages from Western New South Wales. *Technical Reports of the Australian Museum, Online* 23, 45–57. <https://doi.org/10.3853/j.1835-4211.23.2011.1569>.
- Douglass, M.J., Holdaway, S.J., Fanning, P.C., Shiner, J.I., 2008. An assessment and archaeological application of cortex measurement in lithic assemblages. *Am. Antiq.* 73, 513–526.
- Douglass, M.J., Holdaway, S.J., Shiner, J., Fanning, P.C., 2016. Quartz and silcrete raw material use and selection in late Holocene assemblages from semi-arid Australia. *Quarter. Int. New Approaches Study Quartz Lithic Industries* 424 (December), 12–23. <https://doi.org/10.1016/j.quaint.2015.08.041>.
- Douglass, M.J., Lin, S.C., Braun, D.R., Plummer, T.W., 2018. Core Use-life distributions in lithic assemblages as a means for reconstructing behavioral patterns. *J. Archaeol. Method Theor.* 25 (1), 254–258. <https://doi.org/10.1007/s10816-017-9334-2>.
- Driscoll, K., 2011. Vein quartz in lithic traditions: an analysis based on experimental archaeology. *J. Archaeol. Sci.* 38 (3), 734–745. <https://doi.org/10.1016/j.jas.2010.10.027>.
- Egloff, B.J., 1973. A method for counting ceramic Rim Sherds. *Am. Antiq.* 38 (3), 351–353. <https://doi.org/10.2307/279724>.
- Eren, M.I., Diez-Martin, F., Dominguez-Rodrigo, M., 2013. An empirical test of the relative frequency of bipolar reduction in beds VI, V, and III at Mumba Rockshelter, Tanzania: Implications for the East African middle to late stone age transition. *J. Archaeol. Sci.* 40 (1), 248–256. <https://doi.org/10.1016/j.jas.2012.08.012>.
- Faith, J.T., 2007. Changes in reindeer body part representation at Grotte XVI, Dordogne, France. *J. Archaeol. Sci.* 34 (12), 2003–2011. <https://doi.org/10.1016/j.jas.2007.01.014>.
- Faith, J.T., Gordon, A.D., 2007. Skeletal element abundances in archaeofaunal assemblages: economic utility, sample size, and assessment of carcass transport strategies. *J. Archaeol. Sci.* 34 (6), 872–882. <https://doi.org/10.1016/j.jas.2006.08.007>.

- Flenniken, J.J., White, J.P., 1985. Australian flaked stone tools: a technological perspective. *Rec. Aust. Mus.* 36, 131–151.
- Gurtov, A.N., Buchanan, B., Eren, M.I., 2015. 'Dissecting' quartzite and basalt bipolar flake shape: a morphometric comparison of experimental replications from Olduvai Gorge, Tanzania. *Lithic Technol.* 40 (4), 332–341. <https://doi.org/10.1179/2051618515Y.0000000013>.
- Gurtov, A.N., Eren, M.I., 2014. Lower paleolithic bipolar reduction and hominin selection of quartz at Olduvai Gorge, Tanzania: what's the connection? *Quater. Int. Evol. Hominin Behav. Oldowan-Acheulian Transit. Recent Evidence Olduvai Gorge Peninj (Tanzania)* 322–323 (February), 285–291. <https://doi.org/10.1016/j.quaint.2013.08.010>.
- Hagstrum, M.B., Hildebrand, J.A., 1990. The two-curvature method for reconstructing ceramic morphology. *Am. Antiq.* 55 (2), 388–403. <https://doi.org/10.2307/281657>.
- Hayden, B., 1980. Confusion in the bipolar world: bashed pebbles and splintered pieces. *Lithic Technol.* 9 (1), 2–7. <https://doi.org/10.1080/01977261.1980.11754456>.
- Hayden, B., 2015. Insights into early lithic technologies from ethnography. *Philos. Trans. Royal Soc. B: Biol. Sci.* 370 (1682), 20140356. <https://doi.org/10.1098/rstb.2014.0356>.
- Hiscock, P., 2015. Dynamics of knapping with bipolar techniques: modeling transitions and the implications of variability. *Lithic Technol.* 40 (4), 342–348. <https://doi.org/10.1179/2051618515Y.0000000021>.
- Holdaway, S.J., Douglass, M.J., 2012. A twenty-first century archaeology of stone artifacts. *J. Archaeol. Method Theor.* 19 (1), 101–131. <https://doi.org/10.1007/s10816-011-9103-6>.
- Holdaway, S.J., Douglass, M.J., 2015. Use beyond manufacture: non-flint stone artifacts from fowlers gap, Australia. *Lithic Technol.* 40 (2), 94–111. <https://doi.org/10.1179/2051618515Y.0000000003>.
- Holdaway, S.J., Douglass, M.J., Davies, B., in Press. The matrix and the nature of archaeological explanation. In: C. Williamson, P. Crook (Eds.), *Archaeology, History, Philosophy and Heritage: Essays in Honour of Tim Murray*. Amsterdam, Springer.
- Holdaway, S.J., King, G.C.P., Douglass, M.J., Fanning, P.C., 2015. Human-environment interactions at regional scales: the complex topography hypothesis applied to surface archaeological records in Australia and North America. *Archaeol. Oceania* 50 (April), 58–69. <https://doi.org/10.1002/arco.5054>.
- Jeske, R.J., 1992. Energetic efficiency and lithic technology: an upper Mississippian example. *Am. Antiq.* 57 (3), 467–481. <https://doi.org/10.2307/280935>.
- Jeske, R.J., Lurie, R., 1993. The archaeological visibility of bipolar technology: an example from the Koster Site. *Midcontinental J. Archaeol.* 131–160.
- Knell, E.J., 2012. Minimum analytical nodules and late Paleoindian Cody complex lithic technological organization at Hell Gap, Wyoming. *Plains Anthropol.* 57 (224), 325–351. <https://doi.org/10.1179/pan.2012.024>.
- Knight, J., 1988. Technological analysis of the Anvil (bipolar) technique. *Lithics: J. Lithic Stud. Soc.* 12, 57–87.
- Kuijt, I., Prentiss, W.C., Pokotylo, D.L., 1995. Bipolar reduction: an experimental study of debitage variability. *Lithic Technol.* 20 (2), 116–127.
- Kuijt, I., Russell, K.W., 1993. Tur Imdai Rockshelter, Jordan: debitage analysis and historic bedouin lithic technology. *J. Archaeol. Sci.* 20 (6), 667–680. <https://doi.org/10.1006/jasc.1993.1041>.
- Lin, S.C.H., Douglass, M.J., Holdaway, S.J., Floyd, B., 2010. The application of 3D laser scanning technology to the assessment of ordinal and mechanical cortex quantification in lithic analysis. *J. Archaeol. Sci.* 37 (4), 694–702. <https://doi.org/10.1016/j.jas.2009.10.030>.
- Lin, S.C.H., Douglass, M.J., Mackay, A., 2016. Interpreting MIS3 artefact transport patterns in Southern Africa using cortex ratios: an example from the Putselaagte Valley, Western Cape, South African. *Archaeol. Bull.* 71 (204), 173.
- Lin, S.C.H., McPherron, S.P., Dibble, H.L., 2015. Establishing statistical confidence in cortex ratios within and among lithic assemblages: a case study of the middle Paleolithic of Southwestern France. *J. Archaeol. Sci.* 59 (July), 89–109. <https://doi.org/10.1016/j.jas.2015.04.004>.
- Lin, S.C.H., Peng, F., Zwyns, N., Guo, J., Wang, H., Gao, X., 2019. Detecting patterns of local raw material utilization among informal lithic assemblages at the late paleolithic site of Shuidonggou Locality 2 (China). *Archaeol. Res. Asia* 17 (March), 137–148. <https://doi.org/10.1016/jара.2018.11.003>.
- de Lombera-Hermida, A., Rodríguez-Álvarez, X.P., Peña, L., Sala-Ramos, R., Despriée, J., Moncel, M.-H., Gourcinault, G., Voinchet, P., Falguères, C., 2016. The lithic assemblage from Pont-de-Lavaud (Indre, France) and the role of the bipolar-on-anvil technique in the lower and Early Middle Pleistocene Technology. *J. Anthropol. Archaeol.* 41 (March), 159–184. <https://doi.org/10.1016/j.jaa.2015.12.002>.
- Mgeladze, A., Lordkipanidze, D., Moncel, M.-H., Despriée, J., Chagelishvili, R., Nioradze, M., Nioradze, G., 2011. Hominin occupations at the Dmanisi Site, Georgia, Southern Caucasus: raw materials and technical behaviours of Europe's First Hominins. *J. Hum. Evol.* 60 (5), 571–596. <https://doi.org/10.1016/j.jhevol.2010.10.008>.
- Morales, J.I., 2016. Distribution patterns of stone-tool reduction: establishing frames of reference to approximate occupational features and formation processes in paleolithic societies. *J. Anthropol. Archaeol.* 41 (March), 231–245. <https://doi.org/10.1016/j.jaa.2016.01.004>.
- Muller, L.D., 1977. Density determination. In: Zussman, J. (Ed.), *Physical Methods in Determinative Mineralogy*. Academic Press, London.
- Nelson, M.C., 1991. The study of technological organization. *Archaeol. Method Theor.* 3, 57–100.
- Openshaw, S., 1983. The Modifiable Areal Unit Problem. *Concepts and Techniques in Modern Geography* 38. Geo Books, Norwich.
- Orton, J., 2004. The Quartz Conundrum : Understanding the Role of Quartz in the Composition of Late Pleistocene and Holocene Lithic Assemblages from the Verlorenvlei Area, Western Cape. Thesis, University of Cape Town, M.A <https://open.uct.ac.za/handle/11427/7418>.
- Pargeter, J., 2016. Lithic miniaturization in late pleistocene Southern Africa. *J. Archaeolog. Sci.: Rep.* 10 (December), 221–236. <https://doi.org/10.1016/j.jasrep.2016.09.019>.
- Pargeter, J., Eren, M.I., 2017. Quantifying and comparing bipolar versus freehand flake morphologies, production currencies, and reduction energetics during lithic miniaturization. *Lithic Technol.* 42 (2–3), 90–108. <https://doi.org/10.1080/01977261.2017.1345442>.
- Pargeter, J., de la Peña, P., 2017. Milky quartz bipolar reduction and lithic miniaturization: experimental results and archaeological implications. *J. Field Archaeol.* 42 (6), 551–565. <https://doi.org/10.1080/00934690.2017.1391649>.
- Parker, D., 2012. *The Complexity of Lithic Simplicity: Computer Simulation of Lithic Assemblage Formation in Western New South Wales, Australia*. The University of Auckland, M.A., Auckland.
- Partel, Y., Ohel, M., 1981. Measuring the radius of flake bulbs by a spherometer. *Lithic Technol.* 10 (2–3), 28–31. <https://doi.org/10.1080/01977261.1981.11754481>.
- Patterson, L.W., 1979. Additional comments on bipolar flaking. *Flintknapper's Exchange* 2 (3), 21–22.
- de la Peña, P., 2015a. A qualitative guide to recognize bipolar knapping for flint and quartz. *Lithic Technol.* 40 (4), 316–331. <https://doi.org/10.1080/01977261.2015.1123947>.
- la Peña, P., 2015. The interpretation of bipolar knapping in African stone age studies. *Curr. Anthropol.* 56 (6), 911–923. <https://doi.org/10.1086/684071>.
- Phillipps, R.S., 2012. Documenting socio-economic variability in the Egyptian neolithic through store artefact analysis. Ph.D. Dissertation, Auckland, The University of Auckland.
- Phillipps, R.S., Holdaway, S.J., 2015. Estimating core number in assemblages: core movement and mobility during the Holocene of the Fayum, Egypt. *J. Archaeol. Method Theor.* May, 1–21. <https://doi.org/10.1007/s10816-015-9250-2>.
- Powers, M.C., 1953. A new roundness scale for sedimentary particles. *J. Sediment. Res.* 23 (2), 117–119. <https://doi.org/10.1306/D4269567-2B26-11D7-8648000102C1865D>.
- Proffitt, T., de la Torre, I., 2014. The effect of raw material on inter-analyst variation and analyst accuracy for lithic analysis: a case study from Olduvai Gorge. *J. Archaeol. Sci.* 45, 270–283.
- R Development Core Team, 2017. R: A Language and Environment for Statistical Computing (version 3.4.3). Vienna: R Foundation for Stastical Computing. ISBN 3-900051-07-0 (<http://www.R-project.org>).
- Reeves, J.S., 2019. Digital Stone Age Visiting Cards: Quantitative Approaches to Early Pleistocene Hominin Land-Use. Ph.D. Dissertation, Washington, D.C., George Washington University.
- Rezek, Z., Holdaway, S.J., Olszewski, D.I., Lin, S.C., Douglass, M., McPherron, S., Iovita, R., Braun, D.R., Sandgathe, D., 2020. Aggregates, formational emergence, and the focus on practice in stone artifact archaeology. *J. Archaeol. Method Theory* February. <https://doi.org/10.1007/s10816-020-09445-y>.
- Sánchez Yustos, P., Diez-Martín, F., Díaz, I.M., Duque, J., Fraile, C., Domínguez, M., 2015. Production and use of percussive stone tools in the early stone age: experimental approach to the lithic record of Olduvai Gorge, Tanzania. *J. Archaeol. Sci.: Rep.* 2 (June), 367–383. <https://doi.org/10.1016/j.jasrep.2015.03.005>.
- Shott, M.J., 1989. Bipolar industries: ethnographic evidence and archaeological implications. *North Am. Archaeol.* 10 (1), 1–24. <https://doi.org/10.2190/AAKD-X5Y1-89H6-NJGW>.
- Shott, M.J., 1999. On bipolar reduction and splintered pieces. *North Am. Archaeol.* 20 (3), 217–238. <https://doi.org/10.2190/OVP5-TT1E-3WLC-9RCA>.
- Tallavaara, M., Manninen, M.A., Hertell, E., Rankama, T., 2010. How flakes shatter: a critical evaluation of quartz fracture analysis. *J. Archaeol. Sci.* 37 (10), 2442–2448. <https://doi.org/10.1016/j.jas.2010.05.005>.
- Warner, D.J., 1998. Spherometer. In: Bud, R., Warner, D.J. (Eds.), *Instruments of Science: An Historical Encyclopedia*. Taylor & Francis, London, pp. 569–570.
- Whallon, R., 1969. Rim diameter, vessel volume, and economic prehistory. *Michigan Acad.* 11 (2), 89–98.